Three-electron systems with inner-shell vacancies

Micheal J. Conneely
Mathematical Physics Department, University College, Galway, Ireland

Lester Lipsky
Department of Computer Science and Engineering, The University of Connecticut, Storrs, Connecticut 06269

Arnold Russek
Physics Department, The University of Connecticut, Storrs, Connecticut 06269
(Received 27 January 1992)

A computational method is described for obtaining inner-shell-vacancy states of three-electron atoms which combines a block-diagonalization procedure with generalized Feshbach projection operators applicable to systems with three or more electrons. Typically, the accuracy is about 1.5 parts per thousand ($\delta E/E \approx 1.5\times 10^{-3}$). The strength of the method is that it provides many energy levels for each Rydberg series. A quantum-defect analysis is then applied that identifies the members of each series and yields reliable quantum defects and series limits. The method is particularly important in symmetries for which multiple Rydberg series exist. The present work reports on ${}^4P^e$ states of three-electron systems with $3 \le Z \le 10$, which are compared with other calculations. The energies of ${}^2S^e$ states of C^{3+} are also presented as an example requiring both the multielectron Feshbach projection operators and the quantum-defect analysis developed here. Four distinct Rydberg series are found for this case and their series limits obtained.

PACS number(s): 32.30.−r, 32.80.Dz, 31.50.+w, 31.20.Tz

I. INTRODUCTION

Inner-shell-vacancy states, the existence of which was known experimentally in the early 1930s, appear as discrete energy levels embedded in a continuum spectrum. They play an important role in various physical processes such as dielectric recombination, photoabsorption, electron scattering, and multielectron phenomena in ion-atom and atom-atom collisions, to name just a few. The investigation of these states both experimentally and theoretically has yielded important information on the effects of electron correlations in atomic systems. This in turn has led to the development of new theories, classification schemes, and the search for new quantum numbers to characterize these states [1]. The present work describes a computational method for obtaining inner-shell-vacancy states of three-electron atoms that combines a block-diagonalization procedure with Feshbach projection operators. Typically, this method provides energy values that are too high by about 1.5 parts per thousand ($\delta E/E \approx 1.5\times 10^{-3}$). The error is almost entirely due to the absence of continuum functions in the basis set, a limitation imposed by the matrix-diagonalization techniques employed in this work. This question is more completely addressed in Sec. IV B. The value of the method rather lies in providing ten or more energy levels of comparable accuracy for each series within a given configuration. Thus, reliable quantum defects and series limits can be (and are) calculated.

For configurations with multiple series converging to different thresholds, it is extremely difficult to unscramble the different series, particularly if the thresholds are not accurately known. Because the computational method developed in this work generates many members of each series, they can be identified by examining their quantum defects after the threshold values have been determined. Results for all Rydberg series for lithiumlike atoms with $3 \le Z \le 10$ will appear in a subsequent paper; the present work reports the ${}^4P^e$ states, for which comparisons can be made with other works, and a sample multiple Rydberg series for C^{3+} to illustrate the method. The quartet states can be calculated without the Feshbach projection operators developed in this work because they are separated from the ionized states by different spins. They are therefore not coupled by the model Hamiltonian, which contains kinetic and Coulomb terms only. Because they are coupled to the background continuum only via the very small spin-orbit and spin-spin terms in the true Hamiltonian, which are always neglected in structural calculations, they are very long lived and are called *metastable states.*

Inner-shell-vacancy states are not true discrete (normalizable) states. In most cases, they are coupled to the continuum background via the interelectron Coulomb interaction. Generally, the coupling is weak, so that the states behave experimentally very much like true bound states. Nevertheless, they are *not* eigenstates of the physically correct atomic Hamiltonian (as opposed to simplified models of the Hamiltonian used in most computational procedures), and are therefore not stationary states. If they do not first decay via some other deexcitation channel, they must undergo a transition into the background ionization continuum. To obtain these autoionizing states via some calculational procedure, they

must in some way be separated from the background ionization continuum. The two most successful methods devised to accomplish that task are Feshbach projection operators [2] and the complex rotation method [3]. The present work deals exclusively with the former, and extends and generalizes the Hahn, O'Malley, and Spruch [4] version of the Feshbach projection operators.

In the independent-particle model, an atomic state is characterized by its configuration and symmetry, described by the quantum numbers L,S,L_z,S_z,π or J,J_z,π plus the principal and angular quantum numbers of the individual electrons. The wave function that describes the state is the antisymmetrized product of single-electron functions, or linear combinations thereof. Thus, the situation in which a particular core electron is excited, thereby leaving a vacancy in the inner shell, is easily visualized. An atom in such a state will have an energy that in general exceeds the ionization energy. In such situations, or with the simultaneous excitation of two or more outer electrons to large distances from the residual ion, correlation effects become important, since the dominant role of the nuclear Coulomb potential is reduced. Electron correlations are described within the independent-particle model by the superposition of configurations of the same symmetry. For example, the lowest doubly excited $^3S^e$ state (i.e., with two $1s$ vacancies) in helium, $(2,3a)^3S^e$ in the empirical classification of Conneely and Lipsky [5], is composed over 90% of configurations coherently mixed according to $|2sns\rangle + |2pnp\rangle$. Since two-electron atoms are the simplest systems in which multiple excitations can occur, they are the most extensively investigated and have served as prototypes for the spectroscopy of multiple excitations. Several other classification schemes have been used to describe angular and radial correlations in doubly excited states of two-electron systems, two of which are group theoretical: one introduced by Wulfman [6] and used extensively by Sinanoglu and Herrick [7], and the hyperspherical approach first described by Macek [8] and developed by Lin [9] and by Fano and Rau [10].

The concepts and techniques used in the study of doubly excited two-electron systems are relevant to analogous phenomena in atoms with three or more electrons. Such phenomena are far more varied in atoms for which the excited electrons can exchange energy and angular momentum with ionic cores that include other electrons. Transitions from some quartet states, for which Coulomb autoionization decay is forbidden by spin selection rules, were already observed in optical spectra in the 1920s [11]. Since then, the amount of data on multiexcited atomic systems has grown explosively. There are so many observed levels that their identification seems close to impossible, particularly since there have been very few calculations performed beyond the lowest levels. Many reviews have covered studies of multiply excited states [12–15], and recently Mannervik [16] has reviewed developments for few-electron systems with emphasis on emission spectroscopy, while also giving some historical background.

The energy spectrum of lithiumlike ions can be divided into three groups of levels. The first group, converging on the $(1s)^2\,{}^1S^e$ ground state of the corresponding two-electron residual ion, consists of levels with a filled $1s$ shell together with one excited electron. They are the ground state and singly excited states $(1s)^2nl\,{}^2l$ with parity $(-1)^l$. These are shown for Li on the left-hand side of Fig. 1. The second group is composed of levels for which there is only one $1s$ electron. The terminology for these states is not uniform. Either of two electrons can decay down to fill the $1s$ vacancy. Hence, in analogy with two-electron systems, they are often referred to as *doubly excited states.* The other term used to describe inner-shell-vacancy states is taken from the Auger effect for many-electron systems, where it is referred to as a *single-inner-shell-vacancy state.* A representative sample for Li is shown in the center of Fig. 1. The third spectral group consists of *double-K-shell-vacancy states* with *no* electrons in the $1s$ shell. These are also described as *triply excited states.* A representative sample of such states is shown on the right-hand side of Fig. 1.

The singly excited states are well studied experimentally by optical spectroscopy methods and theoretically by various approximations of atomic theory. The levels of the second and third groups, in addition to radiative decay channels, also have nonradiative paths. These states are degenerate with a continuum of states of the atomic Hamiltonian having the same quantum numbers [17], and are called *autoionizing states.* The discrete and continuous states mix to allow the radiationless transition to occur. The selection rules for such a decay require, however, that the total angular momentum J and parity π be

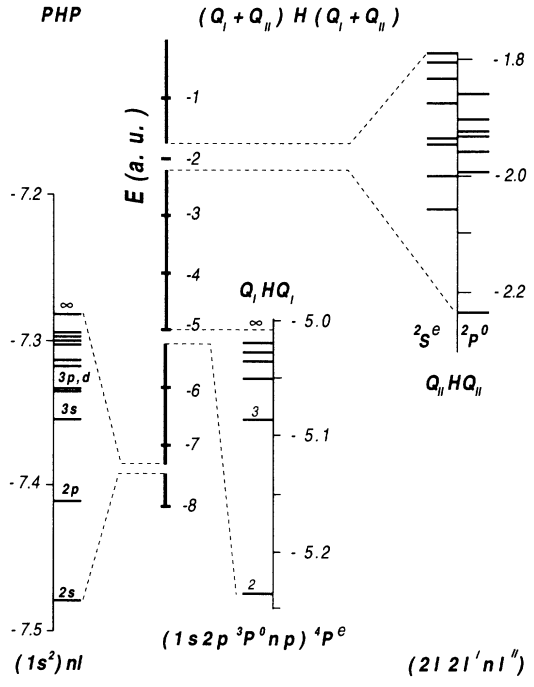

FIG. 1. Energy-level diagram for Li singly excited states, $(1s2pnp)^4P^e$ doubly excited states converging to $1s2p\,{}^3P^o$ threshold, and triply excited $^2S^e$ and $^2P^o$ states converging to various $2l2l'$ thresholds.

conserved. Since we are considering states in the L-S coupling approximation, the selection rules also require that L and S are conserved. Due to the conservation laws for L, S, and π, many multiply excited states are forbidden to decay via the Coulomb interaction. Such states are metastable, and can only decay radiatively or autoionize via the spin-orbit, spin–other-orbit, or spin-spin interactions. These decay modes are slow compared with Coulomb-mediated autoionization ($10^{4}-10^{-9}$ sec versus 10^{-13} sec). The $1s(2p)^2\,{}^4P^e$ and the $(2p)^3\,{}^4S^o$ states of Li-like ions are two specific examples of multiply excited metastable states. The ${}^4P^e$ state is degenerate only with the doublet continuum $[(1s)^2\,{}^1S\,kp]^2P^e$, while the $(2p)^3\,{}^4S^o$ state is embedded in ${}^4S$ continua of the *wrong* parity ($1s2sks\ {}^4S^e$ or $1s2pkp\ {}^4S^e$).

The first accurate calculations on the doubly excited quartet states of lithium were done by Holoien and Geltman [18], who performed variational calculations using Hylleraas-type wave functions, and by Weiss [19], who performed configuration-interaction calculations. Since then, a number of authors have carried out calculations on the lowest quartet and doublet states of lithiumlike ions using a variety of techniques: Lunell and Beebe [20] and Lunell [21] (multiconfiguration Hartree-Fock), Bhatia and Temkin [22,23] (quasiprojection-operator method), Glass [24] and Bunge [25–29] (configuration interaction), Safronova and co-workers [30–32] ($1/Z$ expansion), Chung [33–38] (saddle-point technique). Relativistic and mass-polarization effects are included in Chung's calculations, and the method was also used to calculate the energies of triply excited states [39]. These calculations have been used to identify excited states and Auger lines seen in experiments [40–42]. Chung and Davis [43] have incorporated the saddle-point method with the complex rotation method to calculate the Auger width [44] or the spin-induced width [45] of some atomic ions. Many of these predictions were verified by precise experiments [13,46,47].

Ahmed and Lipsky [48] used a large set of configurations that excluded both $1s$ orbitals to calculate energy levels for some triply excited states of He^- and its isoelectronic sequence. They devised a procedure that automatically sets up all the totally antisymmetric three-electron wave functions for a given set of orbitals (n_1l_1,n_2l_2,n_3l_3) and calculates the matrix elements of the three-electron Hamiltonian using matrix elements already calculated for the two-electron case [49,50]. Their procedure was used in this study to calculate energy levels of three-electron systems with a $1s$ vacancy (i.e., the doubly excited states) for $Z=2-10$ and for all doublet and quartet states with $L=0-4$, some 5000 energy levels all together. Each of the configurations used in the truncated diagonalization procedure has *at most* one electron in the $1s$ shell. As will be shown in Sec. III, this procedure turns out to be an extension of the Hahn, O'Malley, and Spruch [4] version of the Feshbach projection operators [2], which was so successful in predicting doubly excited states in the two-electron case [50–53]. In Sec. IV of this paper, the results for the ${}^4P^e$ states in the isoelectronic series Li to Ne^{7+}, which have but a single Rydberg series, are presented. Section IV also presents a multiple-Rydberg series of states for C^{3+} as an example of an application requiring the generalized version of the Feshbach projection operators. The full catalog of K-shell vacancy states will be published separately. Also in Sec. IV, Rydberg series of levels are fit to effective quantum numbers n^*, the fractional parts of which (the quantum defects) vary slowly with n. To do so, it was found necessary to use threshold energies *shifted* from the values obtained in equivalent two-electron calculations. The reason for this threshold energy shift is established with the help of a perturbation expansion in $1/Z$. It turns out to be an artifact of the calculation, due to the absence of continuum orbitals in the configurations used in the truncated diagonalization procedure.

The generalized Feshbach projection operators here developed are valid for a wide range of metastable or autoionizing states of multielectron atoms, including those involving inner-shell vacancies. They are formulated in Sec. III for three-electron atoms, since three is the smallest number of electrons that illustrate the general formulation. They can be used as they stand for Li-like systems, but for applications involving four or more electrons, a straightforward generalization is required. These projection operators were originally formulated by Russek and Furlan [54] for an unrelated molecular physics application, but are also applicable to autoionizing states.

The present formulation of the Feshbach projection operators is particularly well suited to the matrix block-diagonalization approach, which has been used earlier to obtain autoionizing states [49,50,52,55,56]. Indeed, the formulation of Sec. III places the block-diagonalization approach on a rigorous foundation. However, the present formulation is more general, and permits variational techniques and Z-dependent perturbation theory to be used as well.

II. METHOD

The true physical Hamiltonian describing the system will here be denoted by H_p and is of the form

$$H_p=H+V_s\ , \tag{1a}$$

where V_s stands for a collection of spin-dependent and relativistic terms, all of which are very small, and H is the model Hamiltonian. In its nonrelativistic form in atomic units H is given by

$$H=H_0+V\ , \tag{1b}$$

where

$$H_0=H_1+H_2+H_3=\sum_{i=1}^{3}\left[T_i-\frac{Z}{r_i}\right] \tag{2a}$$

and

$$V=V_{12}+V_{23}+V_{31}\ . \tag{2b}$$

Here T_i is the kinetic-energy operator for the ith electron and $V_{ij}=1/r_{ij}$. The states and energies here described are obtained by diagonalizing the model Hamil-

tonian H using the antisymmetric basis functions $\Psi(n_1l_1,n_2l_2,n_3l_3:LS)$ constructed from hydrogenic functions. The spin-dependent term V_s is mentioned only because it is responsible for the eventual autoionization of so-called *metastable* states, such as quartet states, which are stable against autoionization via the Coulomb interaction (2b), but eventually decay via spin rearrangement.

The procedure described in Ahmed and Lipsky [48] is used for generating the three-electron configurations and the associated matrix of the model Hamiltonian H. A full description of the procedure is given in that work. Following their method, the totally antisymmetric three-electron wave function is expressed in terms of vector-coupled products of all antisymmetric two-electron wave functions $[\Phi_j(1,2|L_j,S_j)]$ constructed from two of the same three orbitals, and multiplied by the wave function of the third electron. That is,

$$\Psi_i(1,2,3)=\sum_j a_{ij}[\phi_j(1,2|L_jS_j)\phi'_j(3)]^{LS} =\sum_j a_{ij}\Phi_j(1,2:3)\ , \tag{3}$$

where $\phi'(\mathbf{r})=R_{nl}(r)Y_l^m(\theta,\phi)\chi^{\mu}_{1/2}$. The Ψ_i are fully antisymmetric, while Φ_j is antisymmetric only in variables 1 and 2. The a_{ij} are the *generalized fractional-parentage coefficients* described in Ref. [48]. They make the linear combination fully antisymmetric in all variables. The nomenclature derives from open-shell theory, where the equivalents to the $\phi_j(1,2|L_j,S_j)$ are referred to as *parents* of the Ψ_i. There may be more than one Ψ_i with the same set of orbitals and the same L,S and π. If so, then a *seniority* index must be assigned to each of the independent functions. Hence the subscript $i=1,2,\ldots$.

The energies are obtained by calculating (in blocks) and diagonalizing a matrix written symbolically as

$$H=aha^T\ , \tag{4}$$

where a is the matrix of the a_{ij}, a^T is its transpose, and h is the matrix whose components are given by

$$h_{ij}=\langle\Phi_i(1,2:3)|3(H_3+1/r_{12})|\Phi_j(1,2:3)\rangle\ . \tag{5}$$

In this way, the two-electron interactions can be calculated in terms of

$$\langle\phi_i(1,2|n_1,l_1,n_2,l_2:L_iS_i)|V_{12}|\phi_j(1,2|n_3,l_3,n_4,l_4:L_j,S_j)\rangle\ ,$$

exactly the matrix elements used in the two-electron problem. The matrix a can be used to construct a representation of the idempotent total antisymmetrization operator A in the basis of the $\Phi_j(1,2:3)$. Note that a is not a square matrix; for a given set of orbitals and configurations, it has the dimensions [number of parents]×[number of independent functions (seniority number)]. It can be shown that

$$aa^T=I\ , \tag{6a}$$

but

$$a^Ta=A\ . \tag{6b}$$

It follows from Eqs. (6) that A is indeed idempotent, since

$$A^2=a^Taa^Ta=a^TIa=a^Ta=A\ . \tag{7}$$

The basis set used in the calculation includes all configurations of the form n_1l_1,n_2l_2,n_3l_3, where $0\le l_i\le l_{\max}=5$ and $n_i\le n_{\max}=20$, with the following restrictions. Only if two of the three n_i are less than or equal to 3 can the third be as large as $n_{\max}$. Otherwise, the maximum value is 6. (For example, the triplets $\{3,3,20\}$ and $\{6,6,6\}$ are included, but $\{2,4,7\}$ is not.) For any configuration, *at most one* n_i can equal 1 (e.g., $\{1,n,1\}$ is not allowed). This latter restriction will be translated into projection-operator terminology (P, $Q_{\rm I}$, and $Q_{\rm II}$ project onto subspaces containing 0, 1, and 2 vacancies in the K shell) in Sec. III.

The procedure yields different numbers of configurations depending on the particular symmetry L,S,π under consideration. For example, for ${}^4S^e$ symmetry, this procedure gives 338 configurations, while for ${}^2D^e$ the number of configurations is 924. Each configuration in turn produces anywhere from zero to ten (or even more) antisymmetric basis functions. For instance, no functions based on $\{2s,2s,2s\}$ are allowed, while $\{2s,2s,2p\}{}^2P^o$ produces but a single function, since the three functions corresponding to the configurations $(2s)^2\,{}^1S\,2p$, $(2s2p)^1P^o2s$, and $(2s2p)^3P\,2s$ all yield the same totally antisymmetric ${}^2P^o$ basis function. On the other hand, $\{1s,2s,2p\}{}^2P^o$ produces two functions, while the 30 configurations consistent with $\{3d,4d,4f\}{}^2F^o$ yield ten orthogonal, independent antisymmetric functions. Since A is idempotent, the number of functions is given by $\mathrm{Tr}(A)$. A computer program automatically generates all the basis functions for a given configuration and also calculates the fractional-parentage coefficients for the basis functions. Further details are provided in Ref. [48].

III. THEORY

A. Formulation of the projection operators

Given a basis set of product states constructed from a fixed set of one-electron orbitals, a class of autoionizing states is obtained by diagonalizing a subspace consisting of configurations, all of which have a single vacancy in the K shell. It will here be shown that this process is completely equivalent to solving for the eigenstates of

$Q_I H Q_I$, where Q_I is a projection operator that rejects all states except those having one, and only one, vacancy in the K shell. For the sake of explicitness, the three-electron case will be considered, since three is the least number of electrons illustrating the general case. The method can be generalized to an arbitrary number of electrons, an arbitrary shell and an arbitrary number of vacancies therein. The form and algebra of projection operators for inner-shell vacancies are essentially the same as those introduced by Russek and Furlan [54], differing only by a notational change to make them consistent with the conventions that have arisen in the literature on autoionizing states. We will show how they reduce to the Hahn, O'Malley, and Spruch projection operators for two-electron atoms. The two-electron situation proves to be too special a case to illuminate the general formulation.

Let ϕ_n be a predetermined set of one-electron spatial orbitals, with ϕ_0 the ground-state (K-shell) orbital. They can be either hydrogenic or Hartree-Fock orbitals. Actually, only ϕ_0 itself is required. The rest of the complete set need not be explicitly obtained if a variational calculation is being carried out. The one-electron projection operators p_i and q_i are defined as

$$p_i = |\phi_0(r_i)\rangle\langle\phi_0(r_i)| \ , \tag{8a}$$

$$q_i = 1 - p_i \ , \tag{8b}$$

where r_i denotes the coordinates of the ith electron. These projection operators satisfy the well-known relations

$$q_i^2 = q_i, \quad p_i^2 = p_i, \quad p_i q_i = 0, \quad p_i + q_i = 1 \ . \tag{9}$$

Projection operators describing different electrons commute:

$$q_i q_j = q_j q_i, \quad p_i q_j = q_j p_i, \quad p_i p_j = p_j p_i \ , \tag{10}$$

from which it follows that all one-electron operators commute (including $j = i$), since q_i and p_i each commute with themselves and $p_i q_i = q_i p_i = 0$.

With three pairs of projection operators, exactly eight product terms can be constructed having a p or a q for each electron. The product of any two of the eight product terms vanishes, since different product terms must differ in the factors for at least one electron. For example,

$$(p_1 q_2 p_3)(p_1 q_2 q_3) = p_1^2 q_2^2 p_3 q_3 = 0 \ . \tag{11}$$

It was shown by Russek and Furlan [54] that these eight products can be grouped into four complementary projection operators:

$$\begin{aligned} R &= p_1 p_2 p_3 \ , \\ P &= q_1 p_2 p_3 + p_1 q_2 p_3 + p_1 p_2 q_3 \ , \\ Q_I &= q_1 q_2 p_3 + q_1 p_2 q_3 + p_1 q_2 q_3 \ , \\ Q_{II} &= q_1 q_2 q_3 \ . \end{aligned} \tag{12}$$

[The notation of Eqs. (12) differs, however, from that of Ref. [54] to conform with the notational conventions adopted to describe autoionizing states.] Each of the projection operators, P, Q_I, Q_{II}, and R is fully symmetric with respect to any permutation of particle coordinates; hence each of them commutes with the antisymmetrization operator. From the commutative property (10) together with Eqs. (9) and (11), it follows that

$$P^2 = P, \quad Q_J^2 = Q_J, \quad \text{and} \quad R^2 = R \tag{13}$$

and

$$P Q_J = R Q_J = R P = Q_I Q_{II} = 0 \ , \tag{14}$$

where the subscript J stands for I or II. It is not difficult to show that

$$P + Q_I + Q_{II} + R = I \ . \tag{15}$$

The projection operators P, Q_I, and Q_{II} project onto subspaces which contain two, one, and zero electrons, respectively, in the K shell. (The subscripts on Q describe the number of *vacancies).* The projection operator R projects onto a subspace containing three electrons in the K shell. Of course, when spin and antisymmetry are introduced, R acting on any antisymmetrized state will give zero. The antisymmetrization operator rejects any configuration that contains three electrons with the same quantum numbers. Consequently, in addition to its other properties, the antisymmetrization operator is a projection operator orthogonal to R.

The eigenfunctions of $Q_I H Q_I$ are those that diagonalize the space consisting of all configurations with a single-K-shell vacancy:

$$Q_I H Q_I \Psi = Q_I H Q_I (Q_I \Psi) = E (Q_I \Psi) \ . \tag{16}$$

Thus if Ψ is an eigenstate of $Q_I H Q_I$, then so is $Q_I \Psi$. Similarly, states with a double vacancy in the K shell are obtained as eigenstates of $Q_{II} H Q_{II}$. The calculations described in Sec. II obtain the eigenstates and eigenenergies of $(Q_I + Q_{II}) H (Q_I + Q_{II})$ rather than just $Q_I H Q_I$. Thus, the calculations do not assume *a priori* that there exist single-K-shell vacancy states and double-K-shell vacancy states. The calculations permit the system to speak for itself, so to speak, and in fact the energy levels do group into single- and double-vacancy states. No energy level is found that would suggest a substantial admixture of single and double vacancies in the K shell.

We now show that the projection operators here described are *Feshbach* projection operators by establishing lower and higher bounds that bracket the fully discrete spectrum of each $Q_J H Q_J$ and locate that bracketed energy range completely within the ionization continuum of H itself. The eigenstates of $Q_J H Q_J$ associated with the fully discrete spectrum are localized and give the autoionizing states.

If the orbital ϕ_0, which generates the projection operators, is an eigenstate of the one-electron Hamiltonian in the field of a bare nucleus,

$$\left(T - \frac{Z}{r} \right) \phi_0 = -\frac{1}{2} \frac{Z^2}{1^2} \phi_0 \ , \tag{17}$$

then lower bounds $E_{L\mathrm{I}}$ and $E_{L\mathrm{II}}$ on the fully discrete spectra of $Q_{\mathrm{I}}HQ_{\mathrm{I}}$ and $Q_{\mathrm{II}}HQ_{\mathrm{II}}$ are easily obtained as the $1s,2l,2l'$ degenerate energy level of

$$H_0=\sum_{i=1}^{3}\left[T_i=\frac{Z}{r_i}\right]=Z^2\mathcal{H}_0 \tag{18}$$

for $E_{L\mathrm{I}}$, and the $2l,2l',2l''$ degenerate energy level for $E_{L\mathrm{II}}$. Thus,

$$E_{L\mathrm{I}}=-\tfrac{1}{2}Z^2\left[\frac{1}{1^2}+\frac{1}{2^2}+\frac{1}{2^2}\right]=-\tfrac{3}{4}Z^2\ , \tag{19a}$$

$$E_{L\mathrm{II}}=-\tfrac{1}{2}Z^2\left[\frac{1}{2^2}+\frac{1}{2^2}+\frac{1}{2^2}\right]=-\tfrac{3}{8}Z^2\ . \tag{19b}$$

These are generous lower bounds, since the positive-definite contributions of the interelectron repulsion terms

$$H'=1/r_{12}+1/r_{23}+1/r_{31}=Z\mathcal{H}' \tag{20}$$

to $E_{L\mathrm{I}}$ and $E_{L\mathrm{II}}$ have been omitted. These bounds need not be the refined bounds sought in a variational calculation of a given energy level. They only have to bracket the fully discrete spectrum of QHQ with sufficient accuracy to show that it lies in the ionization continuum of H above the singly excited states. In all cases, the lower bound (19) is quite adequate to accomplish that task. Thus, no eigenstate of QHQ can converge to an optically excited state in any calculation, even when the basis space is indefinitely enlarged.

The higher bound on the fully discrete spectrum of $Q_{\mathrm{I}}HQ_{\mathrm{I}}$, which signals the onset of the ionized continuum of $Q_{\mathrm{I}}HQ_{\mathrm{I}}$, is the lowest series limit for single vacancy states. For systems controlled by a Coulomb potential, the onset of a continuum is always the series limit of Rydberg series. Consequently, the higher bound is established when the lowest 15 or so levels are fit to a Rydberg series of a form

$$E_n=E_c-\frac{(Z-2)^2}{2(n-d)^2}\ ,$$

where the quantum defect $d(n)$ is a slowly varying function of n, and E_c is the series limit, which should be the energy of the two-electron core state. Together, $E_{L\mathrm{I}}$ and E_c provide a quick and simple range for the energies of single-K-shell-vacancy autoionizing states.

B. The Hahn, O'Malley, and Spruch operators

The three-electron projection operators of Sec. III A are in some sense generalizations of the Hahn, O'Malley, and Spruch projection operators for the two-electron case. In the notation of Sec. III A, the Hahn, O'Malley, and Spruch projection operators P and Q are defined by

$$P=P_{\mathrm{I}}+P_{\mathrm{II}}\ , \tag{21a}$$

$$Q=1-P\ , \tag{21b}$$

where

$$P_{\mathrm{I}}=q_1p_2+p_1+q_2\ , \tag{22a}$$

$$P_{\mathrm{II}}=p_1p_2\ , \tag{22b}$$

and where p and q are given by Eq. (8), with ϕ_0 a $1s$ hydrogenic state in the field of a bare nucleus. The operator P_{I} could equally well have been denoted by Q_{I}, depending on whether the $1s$ shell is regarded as half full or half empty. Since Hahn, O'Malley, and Spruch characterized the autoionizing state (Q space) as having no electron in the $1s$ shell, the single-occupancy case is included in P space. The Hahn, O'Malley, and Spruch projection operator P is more familiarly written in the form

$$\begin{aligned}P&=P_{\mathrm{I}}+P_{\mathrm{II}}=(1-p_1)p_2+p_1(1-p_2)+p_1p_2\\&=p_1+p_2-p_1p_2\ ,\end{aligned} \tag{23a}$$

so that

$$Q=1-P=1-p_1-p_2+p_1p_2=q_1q_2\ , \tag{23b}$$

These projection operators can be easily shown to have adequate bounds $E_L=-Z^2/4$ and $E_U=-Z^2/8$ to separate the fully discrete spectrum of QHQ from the optically excited states (which are in PHP space).

C. Application to lithiumlike atoms

In the three-electron case investigated in this work, a single vacancy in the K shell results in either an autoionizing or a metastable state. As a consequence, the single-vacancy projection operator is here denoted by Q_{I}, consistent with the established convention of having autoionizing states in Q space. The present investigation employs a finite basis set consisting of fully bound eigenstates of H_0, given by (2a). The orbital ϕ_0, which defines the projection operators (8), is the ground hydrogenic state in a Coulomb field Z/r. Figure 1 shows the energy spectrum for neutral lithium decomposed into P, Q_{I}, and Q_{II} subspaces. The solid lines in the spectrum on the left are eigenenergies of PHP, including the ground state as well as optically excited states $(1s^2nl)^2l$, which can only decay via photon emission. The continuum spectrum of PHP commences at $E=-7.280$ a.u., with a $(1s)^2$ residual ion plus a free electron. The spectrum of $Q_{\mathrm{I}}HQ_{\mathrm{I}}$, shown in the center, is bounded from below by $E=-6.75$ a.u., which is the common energy of a degenerate set of eigenstates of H_0 characterized by $1s,2l,2l'$. In addition to H_0, the full Hamiltonian contains the sum of electron-electron repulsive potentials $\sum_{i<j}1/r_{ij}$. Since this latter is a positive-definite operator, its expectation value must always be positive regardless of Ψ, raising the lowest energy in the spectrum of $Q_{\mathrm{I}}HQ_{\mathrm{I}}$ to a value higher than -6.75 a.u. by a substantial amount.

All the eigenstates of $Q_{\mathrm{I}}HQ_{\mathrm{I}}$ between the $(1s)^2$ and $1s2l$ thresholds are autoionizing or metastable states that can decay into the eigenstates of PHP via the interaction term $Q_{\mathrm{I}}H_pP+PH_pQ_{\mathrm{I}}$, where H_p is the true physical Hamiltonian. This latter contains spin-dependent terms collected in V_s in addition to the interelectron Coulomb interaction terms given in Eq. (2b). If the Coulomb terms are able to mediate a transition between Q and P spaces (Coulomb autoionization), the process can be quite rapid.

If the terms in (2b) cannot mediate the transition, the states are termed *metastable*. They are actually eigenstates of the model Hamiltonian H, but will eventually autoionize via spin-dependent terms in V_s such as spin-orbit and spin-spin. However, the process is very slow compared with Coulomb autoionization. In the energy range between the $(1s)^2$ and $1s2l$ thresholds, an outgoing electron is energetically possible only if one of the other electrons simultaneously drops down to fill the vacancy in the $1s$ *shell*. In this sense, the three-electron Hamiltonian $Q_{\rm I}HQ_{\rm I}$ accomplishes exactly what the Hahn, O'Malley, and Spruch Hamiltonian QHQ accomplishes for the two-electron case.

It should be pointed out that the lower bound of -6.75 a.u. to the eigenstates of $Q_{\rm I}HQ_{\rm I}$ is valid even if the configurations are not constructed from pure hydrogenic functions, *provided* that ϕ_0, which defines the one-electron projection operator p, is a pure hydrogenic function. Whatever functions are used, they can be expanded in the complete set of eigenfunctions of H_0, and $Q_{\rm I}$ rejects all eigenfunctions of H_0 with energies below -6.75 a.u. Thus, screened Coulomb radial functions can be employed, or variational procedures can be used to determine the radial functions. Either of these options may yield more accurate results than those obtained here, but at the expense of a vast increase in effort. If, on the other hand, the orbital projection operator p is changed to the ground state of a *screened Coulomb* wave function, the entire problem is changed, and the bounds must be recomputed to validate that the resulting projecting operators are Feshbach.

The eigenspectrum of $Q_{\rm II}HQ_{\rm II}$ (double-K-shell vacancies) starts at even higher energies, $E > -3.375$ a.u., corresponding to the degenerate set of eigenstates of H_0 characterized by $2l,2l',2l''$. These are shown at the right, taken from Ahmed and Lipsky [48].

IV. CALCULATED RESULTS FOR $^4P^e$ STATES

Since the main purpose of this work is to present the method and demonstrate its validity, only two sets of results are presented as examples. The $^4P^e$ states are examples of a symmetry that has but a single Rydberg series. These quartet states are orthogonal to the subspace of the projection operator P, so they are actually eigenstates of the model Hamiltonian given by (1b). As a consequence, projection operators are not needed here. For this reason, many calculations exist for these metastable states with which to assess the accuracy of the present method. The full power of the method is needed in the multiple-Rydberg case for symmetries in which autoionizing states are coupled to the ionized states of H via the Coulomb interactions (2b) in H.

For the set of $\{n_i,l_i\}$ described in Sec. II, the $^4P^e$ symmetry has 524 configurations, from which 694 totally antisymmetric functions are constructed. The 694×694 Hamiltonian matrix is then computed and diagonalized. There is only one Rydberg series of states below any of the four $1s2l$ two-electron states: $1s2s\ ^1S^e$, $1s2s\ ^3S^e$, $1s2p\ ^1P^o$, and $1s2p\ ^3P^o$. It corresponds to the series

$$\{(1s2p)^3P^o\}np\ ^4P^e \quad \text{for } n>2\ .$$

These states happen to be metastable. Since there is no adjacent $^4P^e$ continuum into which they can decay, they are stable against simple Coulomb autoionization. Moreover, there are no quartet singly excited states, so the states are also stable against photodecay.

The Hamiltonian matrix H can be written as

$$H=Z^2\mathcal{H}_0+Z\mathcal{H}'\ , \tag{24}$$

where $\mathcal{H}_0$ and $\mathcal{H}'$ are independent of Z. Therefore, once they have been computed, it is a simple matter to compute H for as many values of Z as desired. Of course, H must be diagonalized anew for each value of Z.

A. The energies

In order to guarantee eight-digit accuracy, all calculations were carried out to at least double precision on the IBM3090 computer at the University of Connecticut Computer Center, which processes numbers to approximately 17 decimal digits. The two-electron matrix elements were computed in quadruple precision on the VAX 8700 computer in the University College, Galway, computer center, since the largest roundoff error is bound to occur in these matrix elements [49]. After calculating the matrix elements described in Eq. (5) for a given Z,L,S,π, the eigenvalues of H [Eq. (4)] were computed. In principle, this involves finding the orthogonal transformation that satisfies

$$U^{-1}HU=\Lambda\ , \tag{25}$$

where Λ is diagonal. The matrix U yields the eigenfunctions $\bar{\Psi}_n(1,2,3;L,S,E_n)$ of H via the relation

$$\bar{\Psi}_n(1,2,3;L,S,E_n)=\sum_i u_{ni}\Psi_i(1,2,3)\ , \tag{26}$$

where the $\Psi_i(1,2,3)$ are the functions from Eq. (3). However, to explicitly compute U would require three times the space and three times the computer CPU time it takes to find Λ alone. Since we are not prepared to examine the wave functions at this time, the simpler course was taken. The resulting energies below total ionization are given (in a.u.) in Table I for $Z=3-10$ for the configuration $^4P^e$. Although there are over 600 energy eigenvalues, only the lowest 10–16 (depending on Z) are physically significant. The cutoff is selected by examining the quantum defects, as described in the next section.

B. The effective quantum numbers and quantum defects

Whenever an atomic system can be viewed as a single electron orbiting a positive ionic core, the energy levels can be parametrized by the Rydberg formula:

$$E_n=E_c-\frac{1}{2}\left[\frac{Z-N_c}{n^*}\right]^2\ , \tag{27}$$

where $Z-N_c\geq1$ is the net charge of the ionic core and n^* is the effective quantum number. What makes this formula so useful is the fact that n^* can be written as

TABLE I. Energy levels (in a.u.) for $(1s2p)^3P^o np\ ^4P^e$ metastable states, for $Z=3-10$.

n \ Z	3	4	5	6	7	8	9	10
2	5.238 42	9.855 19	15.975 79	23.599 59	32.725 85	43.353 91	55.483 28	69.113 62
3	5.088 49	9.414 55	15.103 22	22.154 11	30.567 31	40.342 79	51.480 39	63.979 96
4	5.053 30	9.298 50	14.856 25	21.726 95	29.910 80	39.407 84	50.218 05	62.341 38
5	5.037 77	9.240 76	14.738 89	21.529 46	29.610 44	38.981 44	49.642 49	61.593 69
6	5.030 10	9.213 43	14.679 27	21.424 23	29.447 16	38.747 97	49.326 76	61.183 60
7	5.025 70	9.197 31	14.643 76	21.362 04	29.351 18	38.610 97	49.141 38	60.942 43
8	5.022 93	9.186 98	14.620 96	21.322 13	29.289 57	38.522 94	49.022 15	60.787 16
9	5.021 07	9.179 96	14.605 44	21.294 97	29.247 59	38.462 93	48.940 83	60.681 22
10	5.019 75	9.174 98	14.594 41	21.275 63	29.217 68	38.420 16	48.882 86	60.605 70
11	5.018 79	9.171 31	14.586 28	21.261 37	29.195 62	38.388 59	48.840 07	60.549 95
12	5.018 00	9.168 54	14.580 13	21.250 55	29.178 87	38.364 61	48.807 57	60.507 62
13	5.016 99	9.166 39	14.575 35	21.242 16	29.165 85	38.345 98	48.782 31	60.474 72
14	5.015 35	9.164 67	14.571 57	21.235 50	29.155 53	38.331 21	48.762 29	60.448 64
15		9.162 85	14.568 52	21.230 14	29.147 22	38.319 30	48.746 14	60.427 61
16		9.159 63	14.565 67	21.225 75	29.140 42	38.309 55	48.732 93	60.410 40
17			14.560 78	21.221 22	29.134 63	38.301 47	48.721 98	60.396 14
∞	5.014 39	9.154 20	14.548 16	21.194 17	29.091 26	38.238 98	48.637 11	60.285 49

$$n^*(n)=n-d(n)\ , \tag{28}$$

where n is the orbital quantum number of the outermost electron and where $d(n)$ is a slowly varying function of n. Here, E_c is the total energy of the core. In the present case of a three-electron system, $N_c=2$, and there are four possible cores, corresponding to the singly excited two-electron ions: $(1s,2s)^1S^e$, $(1s,2s)^3S^e$, $(1s,2p)^1P^o$, and $(1s,2p)^3P^o$. The energies of these ions were calculated using basis functions consistent with those used in the three-electron calculations. The results are given in Table II. When these numbers were used for E_c, in Eq. (27), the results for $d(n)$ were unsatisfactory. But Eq. (27) must hold for some value of E_c, so that parameter was varied until a fit was found that made $d(n)$ as smooth as possible. This is not as much a guessing game as it might seem at first, since for $n\geq 10$ or so, $d(n)$ is very sensitive to the value chosen for E_c. In fact, a change of one unit in the fifth decimal digit of E_c causes a change in the fourth decimal digit of $d(n)$. Therefore, it can be assumed that the E_c are accurate to at least five digits after the decimal point. The values obtained for the $(1s,2p)^3P^o$ state, which is the core ion for the $^4P^e$ doubly excited three-electron states, are also given in Table II, together with their differences from the *ab initio* calculations just mentioned. The explanation for these differences is given in the following section, which also demonstrates that these differences should be, and indeed are, a smooth function of $1/Z$.

TABLE II. Threshold energies (in a.u.)

Z	Calculated	Fitted	Diff.
3	5.020 9971	5.014 392	0.006 6051
4	9.164 6542	9.154 205	0.010 4492
5	14.560 4777	14.548 160	0.012 3177
6	21.207 4704	21.194 170	0.013 3004
7	29.105 1384	29.091 260	0.013 8784
8	38.253 2253	38.238 980	0.014 2453
9	48.651 5878	48.637 111	0.014 4768
10	60.300 1408	60.285 485	0.014 6558

Table III gives the quantum defects of the energy levels presented in Table I for all Z from 3 to 10. Note that the mantissas of the numbers are indeed slowly varying functions of n for each Z (i.e., successive values of n^* differ by almost exactly 1). More results could have been included in Table III, but a cutoff was made based on the value of n for which $n^*(n+1)-n^*(n)\gg n^*(n)-n^*(n-1)$, so that the $d(n)$ are no longer slowly varying.

Table IV compares the results of several calculations for the $1s2pnp\ ^4P^e$ states. Because they are exact eigenstates of the model Hamiltonian (1b), these quartet states can be calculated without reference to the Feshbach projection operators developed in this work. Indeed, it is for this very reason that the computations exist; they can be carried out by conventional variational calculations used for nonautoionizing states. The results are presented in Table IV to assess the accuracy of the method developed in the present work. Since the present work does not rely on the fact that quartet states are exact eigenstates of the model Hamiltonian, the errors are expected to be the same for these states as they are for multiple series of doublet states, which require the full strength of the method. Column A lists the results of the present work, using hydrogenic functions. Columns B–E give the results of other investigations. Column B gives the results of Davis and Chung [45], column C the results of Lunell and Beebe [20] and Lunell [21], column D the results of Holoien and Geltman [18], and column E gives the results of Bunge [25]. Comparisons with the best of these calculations show that the percentage error of the present results, $\delta E/E$, remains almost constant. For $Z=3$, $\delta E/E$ varies from 1.4×10^{-3} for the $n=2$ state to 2.1×10^{-3} for the $n=5$ state. As Z increases, the accu-

TABLE III. Effective quantum numbers of $(1s2p)^3P^o np\ ^4P^e$ metastable states for $z=3-10$.

N \ Z	3	4	5	6	7	8	9	10
2	1.493 93	1.689 12	1.775 41	1.823 68	1.854 50	1.875 93	1.891 73	1.903 88
3	2.597 70	2.771 67	2.847 33	2.886 85	2.910 08	2.925 05	2.935 44	2.943 06
4	3.584 92	3.722 98	3.821 82	3.874 99	3.905 43	3.924 23	3.936 64	3.945 25
5	4.624 41	4.807 01	4.857 29	4.884 69	4.906 77	4.923 80	4.936 49	4.945 81
6	5.641 87	5.811 38	5.858 57	5.896 96	5.926 44	5.946 78	5.960 32	5.969 10
7	6.650 28	6.811 68	6.860 73	6.903 31	6.934 81	6.956 18	6.970 31	6.979 29
8	7.654 45	7.811 62	7.862 35	7.906 81	7.939 35	7.961 72	7.976 88	7.986 65
9	8.565 08	8.811 60	8.863 41	8.908 84	8.942 01	8.965 26	9.981 52	8.992 32
10	9.656 18	9.811 68	9.864 15	9.910 10	9.943 60	9.967 52	9.984 83	9.996 67
11	10.656 52	10.811 85	10.864 72	10.910 98	10.944 56	10.968 90	10.987 13	10.999 91
12	11.765 19	11.812 13	11.865 03	11.911 52	11.945 12	11.969 73	11.988 66	12.002 25
13		12.812 46	12.865 47	12.911 96	12.945 46	12.970 13	12.989 58	13.003 78
14		13.827 61	13.865 73	13.912 22	13.945 60	13.970 27	13.990 15	14.004 73
15		15.213 64	14.867 16	14.912 51	14.945 56	14.970 28	14.990 43	15.005 18
16		19.193 72	16.030 18	15.916 44	15.945 58	15.970 22	15.990 57	16.005 31
17			18.884 74	17.196 71	16.976 78	16.971 65	16.990 59	17.005 35

TABLE IV. A comparison of energy-level calculations (in a.u.) for $1s2pnp\ ^4P^e$ states, $Z=3-10$. A, results of the present study using hydrogenic functions; B, results of Davis and Chung [45]; C, results of Lunel and Beebe [20] and Lunell [21]; D, results of Holoien and Geltman [18] E, results of Bunge [25]; F, results of the present study using generalized Laguerre functions.

Z	A	B	C	D	E	F
			$n=2$			
3	5.238 4	5.245 3	5.243 3	5.245 9	5.245 3	5.244 9
4	9.855 2	9.870 7	9.868 4	9.868 8		
5	15.975 8	16.000 3	15.997 6	15.996 8		
6	23.599 6	23.631 7	23.628 4	23.627 2		
7	32.725 9	32.764 0	32.759 9	32.758 7		
8	43.353 9	43.396 9	43.391 8	43.391 0		
9	55.483 3	55.530 2	55.523 8	55.523 9		
10	69.113 6	69.163 8		69.157 5		
			$n=3$			
3	5.088 5	5.096 7	5.094 1	5.093 9	5.096 8	5.095 0
4	9.414 5	9.428 7	9.424 0	9.423 2		
5	15.103 2	15.124 3	15.119 1	15.119 0		
6	22.154 1	22.182 1		22.176 5		
7	30.567 3	30.601 6		30.596 1		
8	40.342 8	40.382 6		40.377 0		
9	51.480 4	51.525 0		51.519 2		
10	63.980 0	64.028 6		64.022 5		
			$n=4$			
3	5.053 3	5.063 9	5.060 7	5.060 7	5.064 1	
4	9.298 5	9.312 4		9.245 7		
5	14.856 2	14.875 3		14.805 3		
6	21.726 9	21.751 4		21.672 4		
7	29.910 8	29.940 5		29.849 3		
8	39.407 8	39.442 4		39.337 6		
9	50.218 1	50.256 9		50.137 4		
10	62.341 4	62.384 0		62.248 5		
			$n=5$			
3	5.037 8		5.046 3	5.050 2		
			$n=6$			
3	5.030 1		5.038 5			

racy improves and becomes less dependent on n. For $Z=10$, $\delta E/E \approx 0.7\times 10^{-3}$ for all n. The primary limitation on the accuracy of the present method is due to the use of hydrogenic functions without the inclusion of continuum hydrogenic functions. A hydrogenic $n=20$ function is of little use in correcting the deficiencies of a hydrogenic $n=2$ orbital in a screened Coulomb setting. Continuum hydrogenic functions are needed for that task, and they are lacking in the present work. Other studies, using basis sets of Slater orbitals, for example, do better than the present hydrogenic basis. To test this interpretation, the lowest few states were recalculated using a basis set of generalized Laguerre functions, which are similar to Sturmian functions, but are orthogonal under a weighting function r^2. They constitute a complete set of normalizable functions and thus incorporate the hydrogenic continuum. These results, shown in column F, are of the quality of the best results. However, the results for higher levels in the Rydberg series obtained with these functions without using parameter variations are very poor. The conclusion thus derived is that artificial functions may do very well for a limited number of low-lying states, but consistent accuracy over an extended Rydberg series is better served with a large basis of hydrogenic states, for which the present method is ideally suited.

Table V presents energies of $^2S^e$ states for C^{3+} as an example of a symmetry with multiple Rydberg series, all of which are coupled to the ionization continuum via the interelectron Coulomb repulsion terms. This case requires both the generalized Feshbach projection operators of Sec. III A and the quantum-defect analysis described in this section. The energy levels of $(Q_{\rm I}+Q_{\rm II})H(Q_{\rm I}+Q_{\rm II})$ for C^{3+} that correspond to single-K-shell-vacancy states are listed in numerical order in column 2. Columns 3, 4, 5, and 6 show the assignments of the levels of column 2 into the four Rydberg series, with the series limits and core configurations shown at the top of each column. The four series are designated as $[(1s2s)^3S^e]ns\ ^2S^e$, $[(1s2s)^1S^e]ns\ ^2S^e$, $[(1s2p)^3P^o]np\ ^2S^e$, and $[(1s2p)^1P^o]np\ ^2S^e$, respectively. Columns 3–6 give the effective quantum number of each state; the fractional part is the quantum defect. It can be seen that the quantum defects are very slowly and very smoothly varying. Any appreciable alteration from the assignments given in Table V would yield sets of quantum defects looking like sets of random numbers. As would be expected, small anomalies in the quantum defects are found in regions where two series intersect, but these are much smaller than the jumps in quantum defects produced by an invalid assignment.

Note that there is only one state with configuration $[1s(2s)^2]^2S^e$. Thus the lowest energy level in Table V (24.034 68 a.u.) is the first member of two series, namely $[(1s2s)^3S^e]2s\ ^2S^e$ and $[(1s2s)^1S^e]2s\ ^2S^e$. The same can be said for the second level (23.249 43 a.u.) regarding $[(1s2p)^3P^o]2p\ ^2S^e$ and $[(1s2p)^1P^o]2p\ ^2S^e$. Note also that as the effective quantum numbers for each series exceed 16, the quantum defects become erratic. This has been acknowledged in the table by replacing such quantum numbers with "—." If the calculated value of an energy level lies above its appropriate threshold, then "***" is used. Finally, it is seen that although the threshold for one series lies in the midst of the levels of series with higher thresholds, the fitting procedure still works well.

C. Explanation of the threshold shifts

In all calculations we have performed, each Rydberg series of energy levels for every Z and every core state exhibited the expected quantum-defect behavior described by Eq. (27). The series limit E_c should be the energy of the two-electron core state. However, in order to fit the calculated energies to a functional dependence of the form (27), the energy of each series limit had to be shifted to a slightly higher energy than that calculated for the two-electron core state by an amount depending only on the quantum numbers of the core state involved (e.g., $1s2p\ ^3P^o$). The differences between the calculated values for $E_c(1s2p\ ^3P^o)$ and the empirically fitted values given in Table II are plotted in Fig. 2 as a function of $1/Z$. The smoothness of the resulting curve validates two ideas: (1) the heuristic method for obtaining E_c is very stable and accurate, and (2) there appears to be a finite limit for $E_c(Z)$ as $1/Z\rightarrow 0$, which in turn implies that a $1/Z$ expansion is valid. As will be demonstrated, some of this shift (if not all) is an artifact of the approximations inherent in the configuration-interaction calculations using only *bound* hydrogenic states. The discussion presented below demonstrates that the shifts would be smaller and may even disappear or change sign were the complete hydrogenic manifold including continuum states used.

For large Z, the interelectron repulsive terms in the Hamiltonian are small compared with the core attraction terms in the ratio $1/Z$, and the configuration diagonalization can be reasonably well approximated by a perturbation expansion. More precisely, the perturbation calculation using only a finite subset of bound-state eigenfunctions of H_0 should render a reasonably good approximation to the result obtained from a full diagonalization using exactly the same finite set of eigenfunctions as basis set. Thus, any effect caused by omitting the continuum

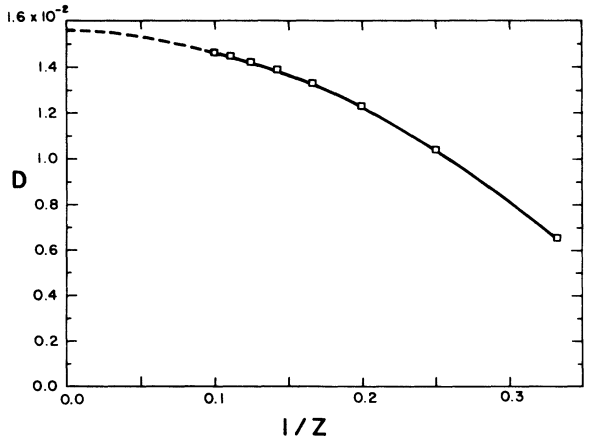

FIG. 2. Differences D of calculated and fitted energies for the $1s2p\ ^3P^o$ threshold as a function of $1/Z$. Data are taken from Table II.

TABLE V. Energy levels (in a.u.) and effective quantum numbers of the four Rydberg series for C^{3+}, $^2S^e$.

	Core state	$(1s2s)^3S^{e\,a}$	$(1s2s)^1S^{e\,b}$	$(1s2p)^3P^{o\,c}$	$(1s2p)^1P^{o\,d}$
I	$-$Energy	ns	ns	np	np
1	24.034 68	1.742 95	1.676 33		
2	23.249 43			1.972 93	1.900 02
3	22.427 24	2.792 37			
4	22.284 34		2.701 05		
5	22.086 95			2.993 46	
6	21.983 16				2.902 27
7	21.943 71	3.840 28			
8	21.770 11		3.706 52		
9	21.750 60	4.785 34			
10	21.692 53			4.006 56	
11	21.634 75	5.853 27			
12	21.576 31				3.838 66
13	21.571 80	6.848 81			
14	21.537 74		4.781 36		
15	21.532 28	7.813 87			
16	21.511 57			5.020 43	
17	21.500 84	8.962 89			
18	21.482 97	9.893 96			
19	21.468 77	10.884 77			
20	21.457 89	11.884 67			
21	21.449 41	12.888 21			
22	21.442 69	13.893 75			
23	21.437 28	14.900 71			
24	21.432 86	15.909 64			
25	21.429 62		5.751 69		
26	21.428 45	—			
27	21.419 99	—			
28	21.413 28			6.042 42	
29	21.383 99	***			
30	21.369 66				4.877 61
31	21.358 30		6.849 94		
32	21.353 74			7.080 70	
33	21.319 97		7.780 10		
34	21.318 09			8.034 85	
35	21.292 61		8.736 71		
36	21.291 60			9.061 66	
37	21.273 98			10.011 71	
38	21.271 97		9.749 37		
39	21.261 99				5.915 85
40	21.259 91			11.031 14	
41	21.255 47		10.872 78		
42	21.249 58			12.015 97	
43	21.245 01		11.825 42		
44	21.241 41			13.013 10	
45	21.236 48		12.819 85		
46	21.234 92			14.011 73	
47	21.229 77		13.807 07		
48	21.229 59			15.029 10	
49	21.225 37			16.013 33	
50	21.224 18		14.828 45		
51	21.220 65			—	
52	21.219 69		15.837 64		
53	21.215 41		—		
54	21.209 25			—	
55	21.206 77		—		
56	21.199 59				6.938 05
57	21.175 63			***	

TABLE V. (*Continued*).

I	Core state −Energy	$(1s2s)^3S^{e\,a}$ ns	$(1s2s)^1S^{e\,b}$ ns	$(1s2p)^3P^{o\,c}$ np	$(1s2p)^1P^{o\,d}$ np
58	21.166 34		***		
59	21.159 37				7.969 01
60	21.133 47				8.941 01
61	21.114 43				9.936 36
62	21.100 30				10.935 00
63	21.089 56				11.935 04
64	21.081 21				12.936 11
65	21.074 58				13.937 87
66	21.069 24				14.940 57
67	21.064 86				15.947 78
68	21.060 32				—
69	21.049 88				—

[a]Series-limit energy is 21.401 25 a.u.
[b]Series-limit energy is 21.187 80 a.u.
[c]Series-limit energy is 21.194 17 a.u.
[d]Series-limit energy is 21.033 40 a.u.

hydrogenic states should also show up in the perturbative treatment, where it will be much more transparent. To understand the shift in the series limit, it is necessary to carry out the expansion to second order in the energy.

For the sake of explicitness, a $(1s2s)$ core (in zeroth order) will be used as an example. The unperturbed states for this case are the single configurations

$$u_n \equiv u_{1s,2s,nl} = |1s,2s,nl\rangle \ , \tag{29a}$$

with energy

$$Z^2\varepsilon_n = -\frac{Z^2}{2}(1/1^2+1/2^2+1/n^2) \ . \tag{29b}$$

To simplify the notation, the entire three-electron configuration is denoted by the single subscript n. Using the notation of Eq. (24), the energy to second order is given by

$$E_n = Z^2\varepsilon_n + Z\mathcal{H}'_{nn} + \sum_{\nu\neq n}\frac{|\mathcal{H}'_{\nu n}|^2}{\varepsilon_n-\varepsilon_\nu} \ . \tag{30}$$

The matrix elements of $\mathcal{H}'$ are independent of Z. Hence, for a fixed electronic state but varying Z (an isoelectronic sequence), successive orders of the perturbation series (30) scale as $Z^2, Z^1, Z^0, \ldots$.

The first-order correction to $Z^2\varepsilon_n$ contains a contribution to the core energy E_c of Eq. (27) that is completely independent of the Rydberg electron, and also a contribution to the second term on the right-hand side of Eq. (27). The contribution to E_c is the same as would be calculated for a pure two-electron core state. Hence it cannot be responsible for a shift in E_c caused by the Rydberg electron. The second term in $\mathcal{H}'_{nn}$ [from Eq. (20)] corrects the leading behavior of the Rydberg energy from $-Z^2/2n^2$ to approximately $-(Z-2)^2/2n^2$. In fact, it accurately corrects for the incomplete screening of the nucleus by the two core electrons. This is clearly not a contribution to E_c. Thus, neither of the two contributions to the first-order correction makes a change in E_n away from E_c as $n\to\infty$.

The second-order correction to $Z^2\varepsilon_n$ can be grouped into three categories. Group I contains all those terms in $\sum_\nu$ that are diagonal in the Rydberg electron state. These terms comprise a second-order contribution to the two-electron core energy plus a contribution from the Rydberg electron that essentially describes polarization of the core by the Rydberg electron, a contribution that must vanish as $n\to\infty$. Neither of these contributions generates a shift in the series limit away from the core energy. Group II contains all of those terms that are neither diagonal in the core states nor the Rydberg states. These group-II intermediate states describe a departure from quantum-defect behavior, and account for the interaction between different Rydberg series. Such effects were indeed seen when accidental very near degeneracies occurred between levels in different Rydberg series with the same L,S,π, and showed up as abrupt departures from smooth quantum-defect behavior.

The energy shift of the series limit arises from the group-III intermediate states: those that are diagonal in the core state. The group-III contribution is of the form

$$\Delta E_{\rm III} = \sum_{n',l'}\frac{|\langle 1s,2s,nl|\mathcal{H}'|1s,2s,n'l'\rangle|^2}{\varepsilon_n-\varepsilon'_n} \ . \tag{31}$$

As $n\to\infty$, all intermediate bound-state Rydberg levels $n'l'$ become lower in energy than ε_{nl}, making all energy denominators positive. Since the numerators are also positive, it follows that $\Delta E_{\rm III}$ is positive. This is the shift in the series limit observed in the configuration-interaction calculation. Confirmation of the correctness of this analysis is obtained by checking the Z dependence of the calculated shifts. The calculated energy shifts obtained from the full diagonalization are plotted in Fig. 2

as functions of $1/Z$. The behavior of the energy shifts for large Z is seen to vary as Z^0 (i.e., independent of Z), as would be predicted for a second-order perturbation term. The calculated shifts exhibit $1/Z$ and $1/Z^2$ dependences arising from perturbations of order higher than 2.

These energy shifts obtained in the configuration-interaction (CI) diagonalization were positive because all of the second-order contributions to ΔE_c were positive. However, were *continuum* hydrogenic states included in the diagonalization, there would be intermediate states with energies higher than $\varepsilon_{\infty l}$. These intermediate states make a negative contribution to $\Delta E_{\rm III}$, which would tend to cancel the positive contribution made by the bound-state configurations. The complete absence of a shift would require a fortuitous exact cancellation of the bound-state contributions by the continuum contributions. Such an exact cancellation is rendered unlikely by the fact that the summation over $n'l'$ in Eq. (31) is dependent upon which states are occupied in the core being considered. Thus, if the cancellation were exact for one particular core, it could not then be exact for other cores.

From Eq. (31) it is seen that the calculated shift in the series limit depends mainly on the core state involved; together with H', the core generates a potential that distorts the Rydberg electron state. Each core state generates its own characteristic potential. On the other hand, since l' is summed over, the dependence of $\Delta E_{\rm III}$ on l should be reduced. However, this derivation does not establish that there should be no variation in shift of the series limit from one Rydberg series to the next for a given core.

V. FURTHER GENERALIZATION OF FESHBACH OPERATORS

If vacancy states are desired in shells other than s shells, as is often the case in Auger state investigations, the single-electron operator p is given by

$$p = \int d^3r' \, R_{nl}(r) R_{nl}(r') \sum_m Y_l^m(\theta,\phi) Y_l^{m\,*}(\theta',\phi') \, , \tag{32}$$

which can be recast more compactly:

$$p = R_{nl}(r) \int d^3r' \, R_{nl}(r') \frac{2l+1}{4\pi} P_l(\Theta_{r,r'}) \, . \tag{33}$$

The angular variables must be included in the definition of the projection operator because the radial functions with different values of l are not mutually orthogonal. The operator p defined in (32) selects any state with given n and l, regardless of its azimuthal quantum number m.

[1] A. R. P. Rau, Rep. Prog. Phys. **53**, 181 (1990).
[2] H. Feshbach, Ann. Phys. (N.Y.) **5**, 357 (1958); **19**, 287 (1962).
[3] A good summary of this method can be found in Y. K. Ho, Phys. Rep. **99**, 1 (1983).
[4] Y. Hahn, T. F. O'Malley, and L. Spruch, Phys. Rev. **134**, B911 (1964).
[5] M. J. Conneely and Lester Lipsky, J. Phys. B **11**, 4135 (1978).
[6] C. Wulfman, Chem. Phys. Lett. **23**, 370 (1973).
[7] O. Sinanoglu and D. R. Herrick, J. Chem. Phys. **62**, 886 (1975).
[8] J. H. Macek, J. Phys. B **1**, 831 (1968).
[9] C. D. Lin, Phys. Rev. A **12**, 493 (1975).
[10] Ugo Fano and A. R. P. Rau, *Atomic Collisions and Spectra* (Academic, New York, 1986).
[11] H. Schuler, Ann. Phys. (Leipzig) **76**, 292 (1925); S. Werner, Nature **118**, 154 (1926).
[12] H. G. Berry, Phys. Scr. **12**, 5 (1975).
[13] T. Andersen and S. Mannervik, Comments At. Mol. Phys. **16**, 185 (1985).
[14] I. Martinson, J. Opt. Soc. Am. B **5**, 2159 (1988).
[15] R. Bruch and K. T. Chung, Comments At. Mol. Phys. **14**, 117 (1984).
[16] S. Mannervik, Phys. Scr. **40**, 28 (1989).
[17] Ugo Fano, Nuovo Cimento **12**, 156 (1935).
[18] E. Holoien and S. Geltman, Phys. Rev. **153**, 81 (1967).
[19] A. Weiss (unpublished).
[20] S. Lunell and N. H. F. Beebe, Phys. Scr. **15**, 268 (1977).
[21] S. Lunell, Phys. Scr. **16**, 13 (1977).
[22] A. K. Bhatia and A. Temkin, Phys. Rev. A **13**, 2322 (1976).
[23] A. K. Bhatia, Phys. Rev. A **18**, 2523 (1978).
[24] R. Glass, J. Phys. B **11**, 3469 (1978).
[25] C. F. Bunge, J. Phys. B **14**, 1 (1981).
[26] C. F. Bunge, Phys. Rev. A **23**, 2060 (1981).
[27] C. F. Bunge, Phys. Rev. A **19**, 936 (1979).
[28] M. Galan and C. F. Bunge, Phys. Rev. A **23**, 1624 (1981).
[29] R. Jauregui and C. F. Bunge, Phys. Rev. A **23**, 1618 (1981).
[30] U. I. Safronova and V. N. Kharitonova, Opt. Spectrosc. **27**, 300 (1967).
[31] U. I. Safronova and V. S. Senashenko, Opt. Spektrosk. **42**, 798 (1977) [Opt. Spectrosc. **42**, 462 (1977)].
[32] L. A. Vainshtein and U. I. Safronova, At. Data Nucl. Data Tables **25**, 311 (1980).
[33] K. T. Chung, Phys. Rev. A **20**, 1743 (1979).
[34] K. T. Chung and B. F. Davis, Phys. Rev. A **22**, 835 (1980).
[35] K. T. Chung, Phys. Rev. A **23**, 2957 (1981).
[36] K. T. Chung, Phys. Rev. A **24**, 1350 (1981).
[37] K. T. Chung, Phys. Rev. A **29**, 682 (1984).
[38] B. F. Davis and K. T. Chung, Phys. Rev. A **29**, 1878 (1984).
[39] K. T. Chung, Phys. Rev. A **25**, 1596 (1982).
[40] M. Rodbro, R. Bruch, and P. Bisgaard, J. Phys. B **12**, 2413 (1979).
[41] R. Bruch, K. T. Chung, W. L. Luken, and J. C. Culberson, Phys. Rev. A **31**, 310 (1985).
[42] R. Bruch, K. T. Chung, E. Trabert, P. H. Heckman, B. Raith, and H. R. Muller, J. Phys. B **17**, 333 (1984).
[43] K. T. Chung and B. F. Davis, Phys. Rev. A **26**, 3278 (1982).
[44] B. F. Davis and K. T. Chung, Phys. Rev. A **31**, 3017 (1985).
[45] B. F. Davis and K. T. Chung, Phys. Rev. A **37**, 111 (1988); **42**, 5121 (1990).
[46] L. Engstrom *et al.*, Phys. Scr. **36**, 250 (1987).
[47] Y. Baudinet-Robinet, H. P. Garnir, and P. D. Dumont,

Phys. Rev. A **34**, 4722 (1986).
[48] Mohamed Ahmed and Lester Lipsky, Phys. Rev. A **12**, 1176 (1975).
[49] Lester Lipsky and A. Russek, Phys. Rev. **142**, 59 (1966).
[50] Lester Lipsky, R. Anania, and M. J. Conneely, At. Data Nucl. Data Tables **20**, 127 (1977).
[51] T. F. O'Malley and S. Geltman, Phys. Rev. **137**, A1344 (1965).
[52] P. L. Altick and E. N. Moore, Phys. Rev. Lett. **15**, 100 (1965).
[53] A. K. Bhatia, A. Temkin, and J. F. Perkins, Phys. Rev. **153**, 177 (1967).
[54] A. Russek and R. J. Furlan, Phys. Rev. A **39**, 5034 (1989).
[55] V. Lopez, A. Macias, R. D. Piacentini, A. Reira, and M. Yanez, J. Phys. B **11**, 2889 (1978).
[56] A. Marcias, F. Martin, A. Riera, and M. Yanez, Phys. Rev. A **36**, 4203 (1987).